Acta Mechanica Slovaca 16 (2): 84 - 90, 2012

* Corresponding author
E-mail address: govardhan_kmtm@yahoo.co.in

Article information
Article history: AMS-Volume16-No.2-00180-12
Received 14 January 2012
Accepted 15 March 2012

Unsteady Boundary Layer Flow of an Incompressible Micropolar Fluid Over a Porous Stretching Sheer

K.Govardhan*, S.Renuka, N. Kishan

Department of mathematics, Osmania University, Hyderabad 500007, A.P, India

KEY WORDS
Unsteady flow, micro polar fluid, stretching surface, skin friction, porous medium.

ABSTRACT
Aim of the paper is to investigate the unsteady boundary layer flow of an incompressible micropolar fluid over a stretching porous sheet when the sheet is stretched in its own plane. The stretching velocity is assumed to vary linearly with the distance along the sheet. Two equal and opposite forces are impulsively applied along axis so that the sheet is stretched, keeping the origin fixed in a micropolar fluid. The governing non-linear equations and their associated boundary conditions are first cast into dimensionless form by a local non-similarity transformation. The resulting equations are solved numerically using the Adams- predictor corrector method for the whole transient from the initial state to final steady- state flow. Numerical results are obtained and a representative set is displaced graphically to illustrate the influence of the various physical parameters on the velocity profiles, microrotation profiles as well as the Skin friction coefficient for various values of the material parameter K. It is found that there is a smooth transition from the small- time solution to the large- time solution. Results for the local skin friction coefficient are presented in table as well as in graph.

1. Introduction

The fluid dynamics over a stretching surface is important in extrusion process. The production of sheeting material arises in a number of industrial manufacturing process and includes both metal and polymer sheets. Examples are numerous and they include the cooling of an infinite metallic plate in a cooling bath, the boundary layer along material handling conveyers, the aerodynamic extrusion of plastic sheets, the boundary layer along a liquid film in condensation process, paper production, glass blowing, metal spinning, and drawing plastic films, to name just a few. The quality of the final product depends on the rate of heat transfer at the stretching surface. A comprehensive review of micropolar fluids mechanically has been presented by Ariman et al [1]. Since the pioneering study by Crane [2] who presented an analytical solution for the steady two – dimensional stretching of a surface in a quiescent fluid, many authors have considered various aspects of this problem and obtained similar solutions. Some mathematical results were presented by many authors, and a good number of references can be found in the papers by Magyari and Keller [8,9]. Sriramulu et.al [14] studied steady flow and heat transfer of a viscous incompressible fluid through porous medium over a stretching sheet.

On the other hand, it is well known that the theory of micropolar fluids has gener-

ated a lot of interest and many flow problems have been studied. The theory of micropolar fluids was originally developed by Eringen [3,4] and has now been applied in the investigation of various fluids. The theory takes into account the microscopic effects arising from the local structure and micromotions of the fluid elements and provides the basis for a mathematical model for non-Newtonian fluids which can be used to analyze the behavoiur of exotic lubricants, polymers, liquid crystals, animal bloods and colloidal or suspension solutions, etc. Since introduced by Eringen many researchers have considerd various problems in micropolar fluids. Nazar et.al [10] studied the stagnation point flow of a non- Newtonian micropolar fluids with zero vertical velocity at the surface or heat generation. Rajeshwari and Nath [12] studied unsteady flow over a stretching surface in a rotating fluid, Noor [11] investigated heat transfer from a stretching sheet.

Guram and Smith [6] investigated the stagnation flows of micropolar fluids with strong and weak interactions. They obtained numerical results using a fourth order Runge – Kutta method. Gorla [5] obtained numerical results by a Runge – Kutta method for the micropolar boundary layer flow at a stagnation point on a moving wall. Heat transfer over a stretching surface with variable surface heat flux in micropolar fluids and MHD stagnation point flow towards a stretching vertical sheet in a micropolar fluid is studied by Ishak et al. [7]. Recently Nazar et al [13] studied the unsteady boundary layer flow of an incompressible micropolar fluid over a stretching sheet. They solved numerically using Keller-box method.

The purpose of the present paper is to study the porous medium effects on the unsteady boundary layer flow of an incompressible micropolar fluid over a stretching sheet when the sheet is stretched in its own plane. A numerical solution is obtained for the governing momentum using the Adams predictor-corrector method.

2. Problem formulation and basic equations

Consider the flow of an incompressible micropolar fluid in the region $y > 0$ driven by a plane surface located at $y = 0$ with a fixed end at $x = 0$. It is assumed that the surface is stretched in the $x-$ direction such that the $x-$ component of the velocity varies linearly along it, i.e. $u_w(x)=cx$, where c is an arbitrary constant and $y > 0$. The simplified two - dimensional equations governing the flow in the boundary layer of a steady, laminar and incompressible micropolar fluids are.

The governing equations of continuity, momentum under the influence of externally imposed transverse magnetic field in the boundary layer laminar and incompressible micropolar fluids are;

$$\frac{\partial u}{\partial x} + \frac{\partial v}{\partial y} = 0, \tag{1}$$

$$\frac{\partial u}{\partial t} + u\frac{\partial u}{\partial x} + v\frac{\partial u}{\partial y} = \left(\frac{\mu + k}{\rho}\right)\frac{\partial^2 u}{\partial y^2} + \frac{k}{\rho}\frac{\partial N}{\partial y} - \left(\frac{\mu + k}{k_p}\right)u, \tag{2}$$

$$\rho j\left(\frac{\partial N}{\partial t} + u\frac{\partial N}{\partial x} + v\frac{\partial N}{\partial y}\right) = \gamma\frac{\partial^2 N}{\partial y^2} - k\left(2N + \frac{\partial u}{\partial y}\right) \tag{3}$$

Subject to the initial and boundary conditions

$$\begin{aligned} &t \le 0: u = v = N = 0, \text{ for any } x, y, \\ &t > 0: v = 0, u = u_w(x) = cx, \\ &N = -n\frac{\partial u}{\partial y} \\ &\text{at } y = 0, \\ &u \to 0, N \to 0, \text{as } y \to \infty \end{aligned} \tag{4}$$

where u and v are the velocity components along the $x-$ and $y-$ axes, respectively, t is time, N is the microrotation or angular velocity whose direction of rotation is in the $x - y$ plane, μ is dynamic viscosity, ρ is density, j is microinertia per unit mass, γ is spin gradient viscosity and k is vortex viscosity. Further, n is a constant and $0 \le n \le 1$. The case $n = 0$, which indicates $N = 0$ at the wall represents concentrated particle flows in which the microelements close to the wall surface are unable to rotate. This case is also known as the strong concentration of microelements. The case $n = 1/2$ indicates the vanishing of anti – symmetric part of the stress tensor and denotes weak concentration of microelements. The case $n = 1$ is used for the modeling of turbulent boundary layer flows. We shall consider here both cases of $n = 0$ and $n = 1/2$.

We introduce the new variables

$$\begin{aligned} &\psi = (cv)^{1/2}\xi^{1/2}xf(\xi, \eta), \\ &N = (c/v)^{1/2}\xi^{-1/2}cxg(\xi, \eta), \\ &\eta = (c/v)^{1/2}\xi^{-1/2}y, \xi = 1 - e^{-\tau}, \tau = ct, \end{aligned} \tag{5}$$

Where Ψ is the stream function defined in the usual way as

$$u = \frac{\partial \psi}{\partial y} \text{ and } v = -\frac{\partial \psi}{\partial x}, \text{and}$$

identically satisfy (1).
Substituting variables (5) in to (2) and (3) gives

$$(1+K)f''' + (1-\xi)\frac{\eta}{2}f'' + \\ + \xi\left(ff'' - f'^2 - \left(\frac{1+K}{\varepsilon}\right)f'\right) + Kg' = \\ = \xi(1-\xi)\frac{\partial f'}{\partial \xi} \qquad (6)$$

$$\left(1+\frac{K}{2}\right)g'' + (1-\xi)\left(\frac{1}{2}g + \frac{\eta}{2}g'\right) + \\ \xi(fg' - f'g) - K\xi(2g+f'') = \\ = \xi(1-\xi)\frac{\partial g}{\partial \xi} \qquad (7)$$

Where K=k/μ is the material parameter. Here γ and are j assumed to be given by $\gamma = \left(\mu + \frac{k}{2}\right)j = \mu\left(1+\frac{k}{2}\right)j$ and $j = \frac{v}{c}$, respectively. The boundary conditions (4) become

$$f(\xi,0) = 0, f'(\xi,0) = 1, g(\xi,0) = -\eta f''(\xi,0), \\ f'(\xi,\infty) = 0, g(\xi,\infty) = 0. \qquad (8)$$

The physical quantity of interest in this problem is the skin friction coefficient C_f which is defined as

$$C_f = \frac{\tau_w}{\rho u^2_w}, \qquad (9)$$

Where τ_w is the skin friction, given by

$$\tau_w = \left[(\mu + K)\frac{\partial u}{\partial y} + kN\right]_{y=0}. \qquad (10)$$

Using variables (5) in (9) and (10), we obtain

$$C_f \mathrm{Re}_x^{1/2} = \xi^{-1/2}[1 + (1-\eta)K]f''(\xi,0). \qquad (11)$$

Further, we can obtain some particular cases of this problem.

A.Early Unsteady Flow

For early unsteady flow $0 < \tau << 1$ we have $\xi \approx 0$, so (6) and (7) reduce in the leading order approximation to

$$(1+K)f''' + \frac{\eta}{2}f'' + Kg' = 0, \qquad (12)$$

$$\left(1+\frac{K}{2}\right)g'' + \frac{\eta}{2}g' + \frac{1}{2}g = 0, \qquad (13)$$

and the boundary conditions (8) become

$$f(0) = 0, f'(0) = 1, g(0) = -\eta f''(0), \\ f'(\infty) = 0, g(\infty) = 0. \qquad (14)$$

B.Final steady- state Flow

For this case, $\xi = 1$ and (6) and (7) take the following forms:

$$(1+K)f''' + ff'' - f'^2 - \left(\frac{1+K}{\varepsilon}\right)f' + Kg' = 0 \qquad (15)$$

$$\left(1+\frac{K}{2}\right)g'' + fg' - f'g - K(2g+f'') = 0 \qquad (16)$$

Subject to the boundary conditions (14).

3. Method of solution

Converting into a system of five first order equations, we have at $\xi + \Delta\xi$, $(y_1 \to f, y_4 \to g)$, $y'_1 = y_2, y'_2 = y_3$, and $y'_4 = y_5$.

Early unsteady flow is obtained by solving these equations with $\xi = 0$. For $\xi > 0$, the above equations reflect a fully implicit scheme with respect to ξ. In both cases, assuming $y_3(\xi,0) = \alpha$ and $y_5(\xi,0) = \beta$, the above system is solved up to $\eta_{\max}(\approx \infty)$.

To solve α and β by Newton –Raphson method.

We need $\frac{\partial y_2}{\partial \alpha}, \frac{\partial y_4}{\partial \alpha}, \frac{\partial y_2}{\partial \beta}$ and $\frac{\partial y_4}{\partial \beta}$ at $\eta = \eta_{\max}$, these quantities are obtained by solutions $y'_1 = y_2, y'_2 = y_3$,

$$y'_3 = \begin{bmatrix} \xi(1-\xi)\dfrac{\partial y_2(\xi+\Delta\xi)}{\Delta\xi} - \\ (1-\xi)\dfrac{\eta}{2}y_3 + \\ \xi(y_1 Y_3 + Y_1 y_3 - 2y_2 Y_2) \\ -ky_5 \end{bmatrix} / (1+k)$$

$y'_4 = y_5$ and

$$y'_5 = \begin{bmatrix} \xi(1-\xi)\dfrac{y_4(\xi+\Delta\xi)}{\Delta\xi} - \\ (1-\xi)\left(\dfrac{1}{2}y_4 + \dfrac{\eta}{2}y_5\right) + \\ \xi(y_1 Y_5 + Y_1 y_5 - y_2 Y_1 - Y_2 y_1) \end{bmatrix} / \left(1+\frac{k}{2}\right)$$

Once with , and another time with

$$y_1(0) = y_2(0) = 0, y_3(0) = 0, \\ y_4(0) = -\eta, y_5(0) = 0 \\ y_1(0) = y_2(0) = 0, y_2(0) = 0, \\ y_3(0) = 0, y_4(1) = 0, y_5(0) = 1.$$

This procedure converging in about three iterations giving correct values of α and β. The system of Ordinary differential equation is solved by Ad-

ams predictor- corrector methods of fourth order. Accuracy is ensured by solving with different $\Delta\xi$, $\eta_{\max}$, $\Delta\eta$.

4. Results and disscussion

The transformed equations (6) and (7) satisfying the boundary conditions (8) were solved numerically using the Adams predictor-corrector method for several values of the material parameter K. Numerical results for Skin friction coefficients, the velocity distribution and microrotation distribution are shown graphically.

To validate our method we have compared the Skin friction coefficients $C_f \mathrm{Re}^{1/2}{}_x$ values with [14] is shown in Table, there is very good agreement between the results when we solved fully unsteady boundary layer equations and final steady state equations.

Computations have been carried out for various values of the n and the material parameters K are represented. The velocity distribution of initial flow (ξ=0) and unsteady flow ($0\leq\xi\leq1$) for various values of K and n is shown. Figs.1, 2 show the resulting dimensionless velocity profiles for various values of K with $n=0$ and $n=1/2$ respectively. From both the figures it is observed that the velocity boundary layer thickness increases with the increasing values of K, for both the cases $n=0$ and $n=1/2$. The figs. 3, 4 represent for final steady state flow (ξ=1) for the cases $n=0$ and $n=1/2$, respectively. It is observed that the velocity increases with the increase of K. The velocity distribution of fully developed unsteady flow ($0<\xi<1$) and final steady state flow (ξ=1) is represented in the figs. 5, 6 for the cases $n=0$ and $n=1/2$, respectively. These figures show that the velocity profiles corresponding to increasing of ξ ($0\leq\xi\leq1$) approach the final steady profile corresponding to ξ=1. It has seen that there is a smooth transition from small time solution (ξ=0) to large time solution (ξ=1).

The effect of porous parameter ε on velocity distribution of initial flow and early unsteady flow (for various ($0<\xi\leq1$) values with $n=0$ and $K=0$ is shown in Fig. 7 and the velocity distribution of final steady state flow (ξ=1) for various ε values with $K=1$, $n=0$ is shown in Fig. 8. It is obvious that existence of porous media ε accecelerates the velocity in both the cases. The magnetic field effect is more in final steady flow.

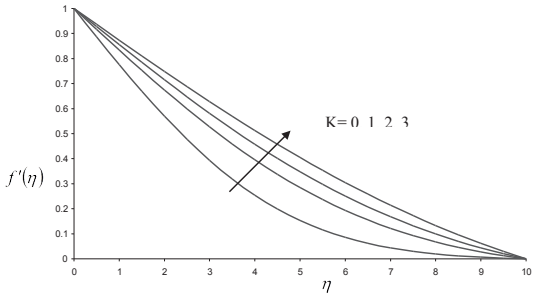

Fig. 1: *Velocity distribution of initial flow (ξ=0) and early unsteady flow ($0<\xi<<1$) for various K with n=0.*

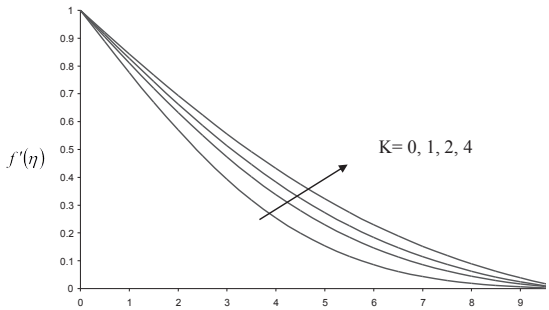

Fig. 2: *Velocity distribution of initial flow (ξ=0) and early unsteady flow ($0<\xi<<1$) for various K with n=1/2.*

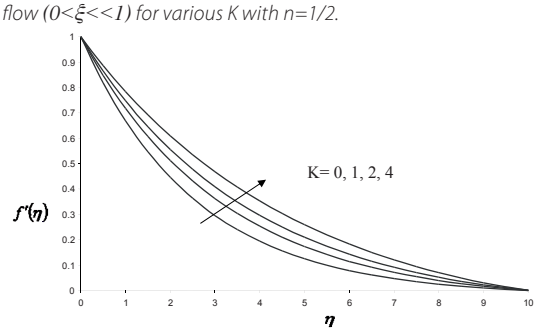

Fig. 3: *Velocity distribution of final steady- state flow (ξ=1) for various K with n=1/2.*

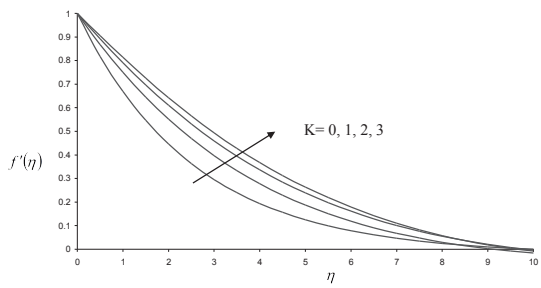

Fig. 4: *Velocity distribution of final steady- state flow (ξ=1) for various K with n=0.*

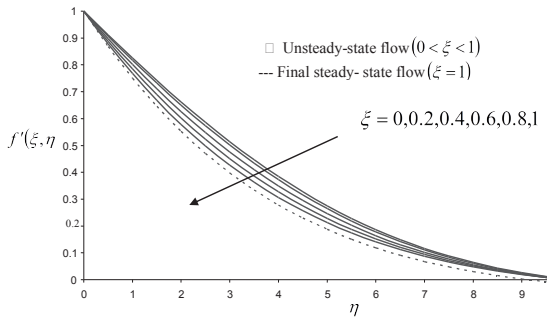

Fig. 5: *Velocity distribution of fully developed unsteady flow for K=1 when n=0.*

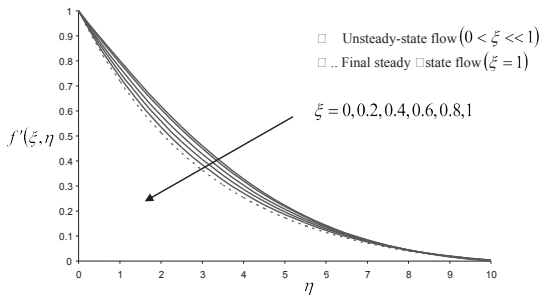

Fig. 6: *Velocity distribution of fully developed unsteady flow for K=1 when n=1/2.*

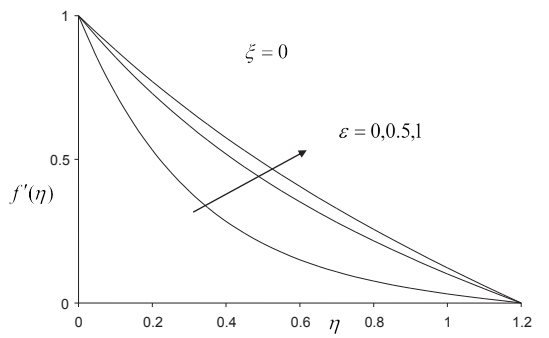

Fig. 7: *Velocity distribution of initial flow (ξ=0) and early unsteady flow (0<ξ≤1) for various ε with n=0 and K=0.*

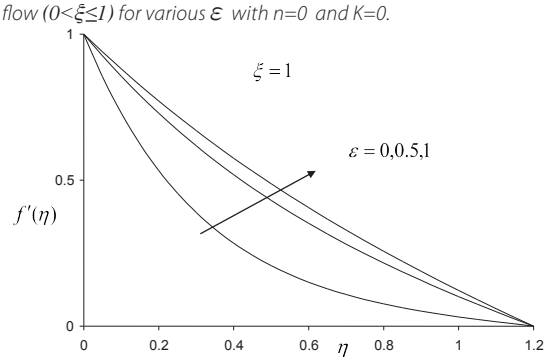

Fig. 8: *Velocity distribution of final steady- state flow (ξ=1) for various ε with n=0 and K=1.*

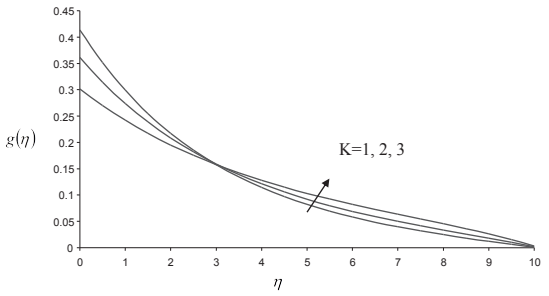

Fig. 9: *Micro rotation distribution of final steady – state flow (ξ=1) for various K when n=1/2.*

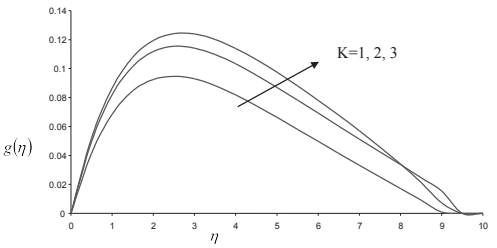

Fig. 10: *Micro rotation distribution of final steady – state flow (ξ=1) for various K when n=0.*

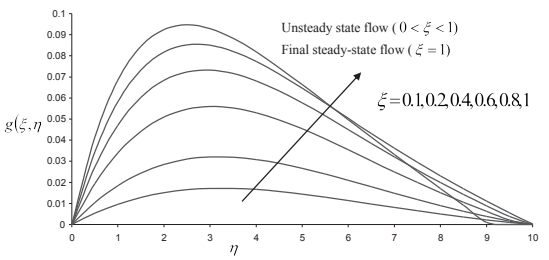

Fig. 11: *Micro rotation distribution of fully developed unsteady flow for n=0 and K=1.*

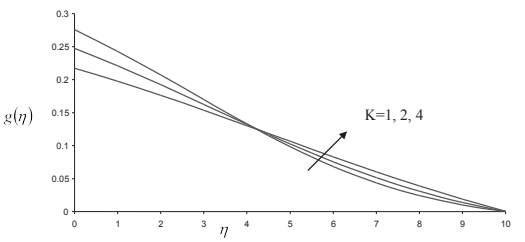

Fig. 12: *Micro rotation distribution of early unsteady flow (0<ξ<<1) for various K with n=1/2.*

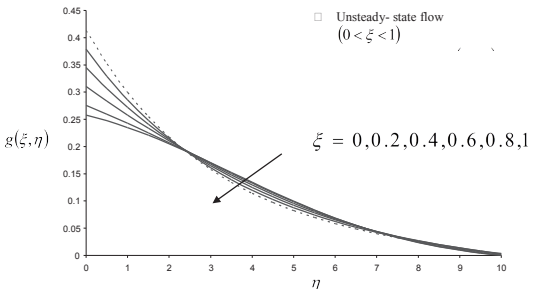

Fig. 13: *Microrotation distribution of fully developed unsteady flow for n=1/2 and K=1.*

microrotation distribution for various values of K, n for steady state and unsteady state flow. The microrotation distribution of final steady state flow (ξ=1) is increases with the increase of the material parameter K is observed from Fig. 9 when $n=0$. The microrotation distribution of final steady state flow (ξ=1) with $n=1$ is shown in Fig. 10 from which the microrotation decreases as K increases in the vicinity of the plate where as it increases as one moves away from it. Fig. 11 represents the microrotation distribution of fully developed unsteady flow for $n=0$ and $K=1$ for $0<\xi\leq1$. It is noticed that the microrotation distribution as parabolic distribution and increases with the increase of ξ. Fig. 12 shows that microrotation distribution of early unsteady flow $(0<\xi\leq1)$ for various K values with $n=1/2$. The microrotation distribution decreases as K increases near the plate but reverse phenomena is observed as one moves away from the plate. The microrotation distribution of fully developed unsteady flow when $K=1$ and $n=1/2$ and final steady state flow (ξ=1) is shown in Fig.13. The microrotation distribution increases near the plate while, the reverse happens far away the plate with the increase of ξ is observed.

Figs.14,15 is drawn for microrotation distribution for final steady state flow (ξ=1) and fully developed unsteady flow with $K=1$, $n=0$ for different porous parameter ε. Due to the porous media effect the microrotation distribution is decreases near the plane and reverse phenomena is observed when it moves far away. It can be seen there is a cross flow at $\eta=5$.

The Skin friction coefficient $C_f \mathrm{Re}^{1/2}{}_x$ with ξ for various values of K is drawn when $n=0$ in Fig. 16 and in Fig.17. It can be seen that the values of decreases as K increases.

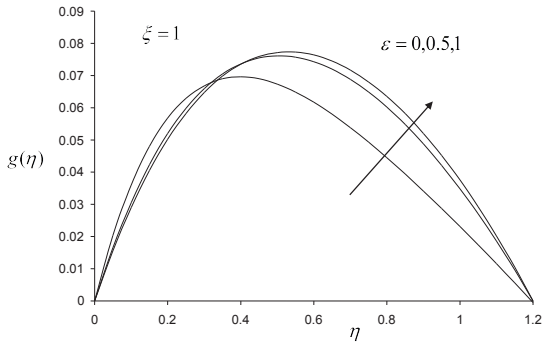

Fig. 14: *Micro rotation distribution of final steady-state flow (ξ=1) for various ε when K=1, n=0.*

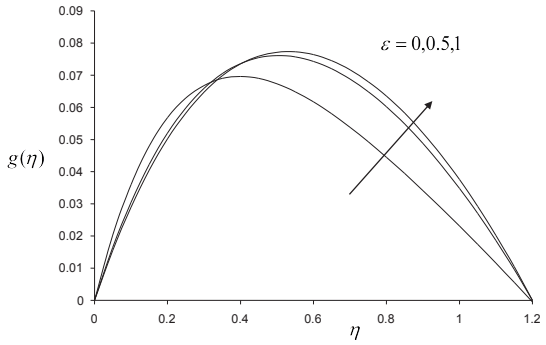

Fig. 15: *Micro rotation distribution of fully developed unsteady flow for various of ε with K=1, n=0.*

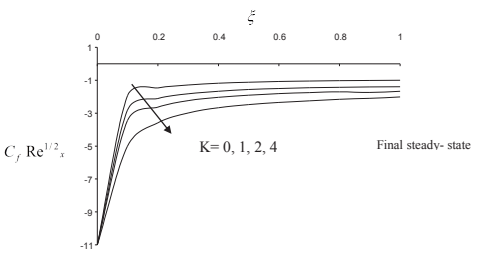

Fig. 16: *Variation with ξ of the skin friction coefficient for various K with n=0.*

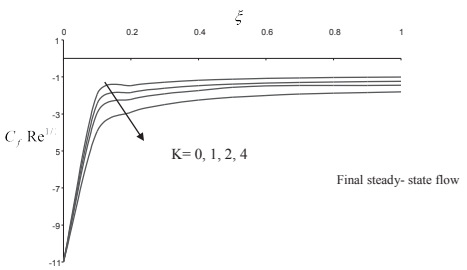

Fig. 17: *Variation with ξ of the skin friction coefficient for various K with n=1/2.*

5. Conclusion

It is clear from the figs that the microrotation effects are more pronounced for $n=1/2$ when compared to those of $n=0$. The microrotation profile for $n=0$ is different as compared to it has a parabolic distribution when $n=0$, where as it has continuously decreasing when $n=1/2$.

The values of the Skin friction coefficients for the final steady flow are shown in Table1. It is noticed that due to impulsive motion, the skin friction coefficients as large magnitude (absolute value) for small time ($\tau \approx 0$ or $\xi \approx 0$) after the start of the motion, and decreases monotonically and reaches the steady state value at $\xi=1$ ($\tau \to \infty$).

Table 1: *Values of the skin friction coefficient* $C_f \mathrm{Re}^{1/2}{}_x$ *for various values of K and* η *when* $\xi=1$.

k/η	0	1/2
0	-1.0043	-1.0043
1	-1.3952	-1.24005
2	-1.6635	-1.4532
4	-2.0092	-1.8105

6. References

[1] Ariman T, Turk M A and Sylvester N.D Microcontinum fluid mechanics-a review", Int j Eng sci,1vol 1, 1973, p. 905-930.

[2] Crane, L.J Flow Past a stretching plane,JournalofAppliedMathematicsand Physics (ZAMP),Vol, 21, 1970. p. 645-647.

[3] Eringen,A.C Simple micropolar fluids. Int. J. Engng. Sci.2. 1964. p.205.

[4] Eringen, A.C,Theory of micropolar fluids. J. Math. Mech 16, 1966.p.1-18.

[5] Gorla, R. S. R Int. J. Engng. Sci 21, p. 25. 1983.

[6] Guram G. S. and A. C. Smith, Comp. Maths. With Appls 6, P.213. 1980.

[7] Ishak, A. Nazar, R. and I. Pop, Heat transfer over a stretching surface with variable surface heat flux in micropolar fluids, Phys. Lett: A 372, p. 559- 561. 2008.[6]

[8] Magyari E. and B. Keller Heat and Mass Transfer in the BoundaryLayers on an ExponentiallyStretching Continuous Surface, Journal of Physics D: Applied Physics 32, 1999.p. 577-586.

[9] Magyari E. and Keller B. Exact Solutions for Self – Similar Boundary–Layer Flows induced by Permeable Stretching Surfaces, European Journal of Mechanics B – fluids 19, 2000, p.109-122.

[10] Nazar, R, Amin, N, Filip, D and Pop I,Stretching point flow of a Micropolar Fluid towards a stretching sheet, Int . J. non- Linear Mech 39, 2004, p1227-1235.

[11] Noor, A, Heat transfer from a stretching sheet, Int J Heat and Mass Transfer.4, 1992, P. 1128- 1131.

[12] Rajeshwari V and Nath G Unsteady flow over a stretching surface in a rotating fluid Int j Eng sci 30, No 6, 1992, p.747-756.

[13] Roslinda Nazr, Anuar Ishak, and Ioan PopUnsteady Boundary Layer Flow Over a Stretching Sheet in a Micropolar Fluid, International Journal of Mathematical, Physical and Engineering Sciences 2(3), 2008. p.161-165.

[14] Sriramulu, A, Kishan, N and Anadarao, J, Steady flow and heat transfer of a viscous incompressible fluid flow through porous medium over a stretching sheet. Journal of Energy, Heat and Mass Transfer 23, 2001, p. 483-495.